

# Differential effects of omega-3 PUFAS on tumor progression at early and advanced stages in TRAMP mice

Gustavo M. Amaro MS<sup>1</sup> | Alana D. T. da Silva MS<sup>1</sup> | Guilherme H. Tamarindo PhD<sup>2</sup> |  
 Celina de A. Lamas PhD<sup>2</sup> | Sebastião R. Taboga PhD<sup>1</sup>  |  
 Valéria Helena Alves Cagnon PhD<sup>2</sup>  | Rejane M. Góes PhD<sup>1</sup> 

<sup>1</sup>Departament of Biological Sciences, Institute of Biosciences, Humanities and Exact Sciences, São Paulo State University (UNESP), São José do Rio Preto, São Paulo, Brazil

<sup>2</sup>Department of Structural and Functional Biology, State University of Campinas (UNICAMP), Campinas, São Paulo, Brazil

## Correspondence

Rejane M. Góes, PhD, Department of Biology Sciences, Institute of Biosciences, Humanities and Exact Sciences, São Paulo State University (UNESP), Rua Cristóvão Colombo, 2265, São José do Rio Preto, SP, Brazil.  
 Email: [rejane.goes@unesp.br](mailto:rejane.goes@unesp.br)

## Funding information

Coordenação de Aperfeiçoamento de Pessoal de Nível Superior, Grant/Award Numbers: Finance Code 001 Alana Della Torre da Silva, Finance Code 001 Guilherme Henrique Tamarindo; Conselho Nacional de Desenvolvimento Científico e Tecnológico, Grant/Award Numbers: 308367/2014-6 Gustavo Matheus Amaro, 311635/2017 Rejane Maira Góes; Fundação de Amparo à Pesquisa do Estado de São Paulo, Grant/Award Numbers: 2019/15109-4 Alana Della Torre da Silva; 2018/21891-4 Rejane Maira Góes;

## Abstract

**Background:** In vitro studies evidenced antitumor effects of omega-3 polyunsaturated fatty acids ( $[n-3]$  PUFAs), but their effects on prostate cancer (PCa) remain controversial in epidemiological studies. Here we investigated whether an  $(n-3)$  PUFA-enriched diet affects tumor progression in transgenic adenocarcinoma of the mouse prostate (TRAMP), at early (12 weeks age) and advanced stages (20 weeks age).

**Methods:** TRAMP mice were fed with standard rodent diet (C12, C20) or  $(n-3)$  PUFA-enriched diet containing 10% fish oil (T12, T20). A group of 8 weeks age animals fed standard diet was also used for comparison (C8). The ventral prostate was processed for histopathological and immunohistochemical analyses and serum samples submitted to biochemical assays.

**Results:** At early stages,  $(n-3)$  PUFA increased the frequency of normal epithelium (3.8-fold) and decreased the frequency of high-grade intraepithelial neoplasia (3.3-fold) and in situ carcinoma (1.9-fold) in the gland, maintaining prostate pathological status similar to C8 group. At advanced stages, 50% of the animals developed a large primary tumor in both C20 and T20, and tumor weight did not differ (C20:  $2.2 \pm 2.4$ ; T20:  $2.8 \pm 2.9$  g). The ventral prostate of T12 and of T20 animals that did not develop primary tumors showed lower cell proliferation, tissue expressions of androgen (AR) and glucocorticoid (GR) receptors, than their respective controls. For these animals,  $(n-3)$  PUFA also avoided an increase in the number of T-lymphocytes, collagen fibers, and  $\alpha$ SMA immunoreactivity, and preserved stromal gland microenvironment.  $(n-3)$  PUFA also lowered serum triglycerides and cholesterol, regulating the lipid metabolism of TRAMP mice.

**Conclusions:**  $(n-3)$  PUFAs had a protective effect at early stages of PCa, delaying tumor progression in TRAMP mice, in parallel with reductions in cell proliferation, AR, and GR and maintenance of the stromal compartment of the gland. However,  $(n-3)$  PUFAs did not prevent the development of primary tumors for the T20 group, reinforcing the need for further investigation at advanced stages of disease.

## KEYWORDS

dietary intervention, docosahexaenoic acid, eicosapentaenoic acid, prostate cancer, steroid receptors, transgenic adenocarcinoma of the mouse prostate

## 1 | INTRODUCTION

Prostate cancer (PCa) is the most frequent cancer in men, with a high mortality rate for cancer-related cases.<sup>1</sup> PCa is a heterogeneous disease with complex etiology, and both molecular and epidemiology studies indicate that diet plays a crucial role in its development.<sup>2</sup> Therefore, the dietary factors have become a relevant subject for cancer prevention,<sup>3</sup> and dietary interventions in patients with cancer are becoming more frequent either to improve therapeutic efficacy or to mitigate nutritional impairment and improve the life quality of patients.<sup>4</sup>

Among the dietary compounds, lipids play a crucial role in prostate homeostasis,<sup>5</sup> and accumulating evidence shows that the lipid nature is an important factor in tissue response and PCa risk.<sup>6,7</sup> Experimental studies evidenced that an intake of saturated fatty acids and omega-6 polyunsaturated fatty acids increases pathological lesions in the gland of rodents and favors PCa progression,<sup>8-10</sup> whereas omega-3 polyunsaturated fatty acids (*(n-3)* PUFAs) have been shown to restrain prostate tumorigenesis.<sup>11,12</sup> Thus, changes in dietary habits by increasing *(n-3)* PUFAs ingestion might be beneficial to prostate histophysiology.

Fish oil is one of the richest sources of the so-called marine omega-3 PUFAs, such as eicosapentaenoic acid (EPA, C20:5) and docosahexaenoic acid (DHA, C22:6).<sup>13</sup> The consumption of DHA and EPA promotes several physiological improvements, especially in cardiovascular diseases, through the modulation of serum lipids.<sup>14</sup> Regarding prostatic health, the chemoprotective action of these PUFAs was observed in androgen-dependent and -independent prostate cell lines through negative regulation of some important oncogenic pathways such as the Akt and NF- $\kappa$ B pathways.<sup>11,15-18</sup> Animal studies have also contributed to highlight the protective role of *(n-3)* PUFAs by reducing tumor growth through the inhibition of tumor-associated macrophage response and recruitment, and modulation of insulin signaling.<sup>19-21</sup> Overall, accumulating evidence suggests that EPA and DHA intake might represent an interesting approach for prostatic disorder management, and epidemiological studies have reported a positive correlation between the intake of these PUFAs and a lower risk of PCa development.<sup>22,23</sup> However, some studies have reported an association between high serum and intraprostatic levels of EPA and DHA and an increased risk of PCa development and poor prognosis,<sup>24-26</sup> raising doubts about the possible role of these PUFAs in PCa chemoprotection. Therefore, more *in vivo* studies are needed to better understand the mechanism of *(n-3)* PUFAs in PCa and to assess its capacity in the chemoprotection of prostatic disorders.

The transgenic adenocarcinoma of the mouse prostate (TRAMP) is a model widely used to study prostatic carcinogenesis.<sup>27-30</sup> The adenocarcinoma is triggered by expression of the large and small T antigen (T/tag) of the simian virus 40 in the prostate epithelium under the control of the rat probasin promoter.<sup>27</sup> TRAMP mice display several hallmarks of human PCa such as the development of androgen-dependent disease and posterior hormone-refractory phenotype,<sup>27-29</sup> constitutive activation of Akt/NF- $\kappa$ B axis,<sup>31</sup> increased lipogenesis,<sup>32</sup> and deregulation of inflammatory signaling.<sup>33</sup>

This transgenic mouse model replicates several parameters of human PCa progression and has been widely adopted to assess new therapies for PCa management.<sup>30</sup> Thus, at 8-weeks of age, the ventral and dorsolateral lobes of the TRAMP prostate gland frequently exhibit low-grade intraepithelial neoplasia (LGPIN), which progresses to high-grade intraepithelial neoplasia (HGPIN) at 12–16-weeks of life. *In situ* carcinoma (CIS) lesions increased from 8-weeks age onwards and poorly differentiated tumors are frequent after 18-weeks of age.<sup>30,34,35</sup> The TRAMP model thus allows us to investigate the impact of several approaches such as dietary interventions in a controlled way on the initial and advanced phases of tumor progression either as a protective or therapeutic agent.

Overall, *in vitro* assays have evidenced the multiple mechanisms underlying antitumor properties of *(n-3)* PUFAs, particularly of DHA.<sup>11,15,18</sup> However, as stated before, the evidence about the protective role of *(n-3)* PUFAs against PCa remains controversial in epidemiological studies, mainly in the advanced stages.<sup>24-26</sup> Here we hypothesized that dietary *(n-3)* PUFA can mitigate PCa severity in TRAMP, investigating whether diet enriched with *(n-3)* PUFA can affect tumor progression in TRAMP mice in early and advanced stages of PCa.

## 2 | MATERIALS AND METHODS

### 2.1 | Experimental design

Male transgenic mice (C57BL/6-Tg [TRAMP] 8247 Ng/J X FVB/Unib) were provided by the Multidisciplinary Center for Biological Investigation from Laboratory Animal Science at the State University of Campinas (UNICAMP) at 7 weeks of age. Two stages of disease were examined: an early stage, at 12 weeks old, when the gland exhibits a high frequency of proliferative disturbance (low- and high-grade intraepithelial neoplasia) and a few foci of localized adenocarcinoma (carcinoma *in situ*), and an advanced stage, at 20 weeks old, when, beyond these pathological alterations, a massive primary tumor can be observed.<sup>27,30</sup> Animals were randomly divided into groups ( $n = 10$  per group), fed with a standard (C12 and C20) or *(n-3)* PUFA-enriched (T12, T20) rodent diet. A group of animals at 8 weeks old (C8,  $n = 10$ ), fed with a standard diet, was also included for comparison, since the proliferative disturbances arises in the gland around this age. Control groups received an AIN-93 diet,<sup>36</sup> while a diet enriched with *(n-3)* PUFA was prepared based on the AIN-93 diet, but replacing 10% of corn scratch with fish oil (containing 5 g of DHA and 1 g of EPA in 10 g of oil) (DHA 500TG; Naturalis<sup>®</sup>) (Tab 1), based on a previous study.<sup>37</sup> The diet of protein (20%), essential fatty acids (7% of soybean oil), and micronutrient (vitamins and minerals) was maintained as recommended for rodents. Furthermore, despite the reduction in carbohydrate content, this diet is not considered to be hypoglycemic.<sup>38,39</sup>

At the end of the experiment, mice were anaesthetized with xylazine hydrochloride (5 mg/kg, intramuscular) and ketamine hydrochloride (60 mg/kg, intramuscular) and euthanized. Ventral prostates were processed for morphological and immunohistochemical

analyses. Animal care and experiments were conducted according to Brazilian guidelines for the care and use of animals for scientific and educational purposes (BDCA)—CONCEA, and were approved by the Ethics Committees on Animal Use (CEUA) of IBILCE/UNESP (Protocol: 198/2018) and UNICAMP (Protocol: 5117-1/2019).

## 2.2 | Biometric and metabolic analyses

The food intake was assessed every 3 days to determine the amount of food (in grams) consumed in a week. Energy intake was calculated by multiplying the food intake by the quantity of energy in each diet. Moreover, the relative weight gain (RW, %) was calculated by the following formula:  $RW = (FW - IW \times 100) / IW$ , where FW means final weight and IW initial weight.

The fasting glucose level (12 h of fasting) was measured through the glucose monitor Accu-Check (Roche Diagnostics). After euthanasia, blood samples were collected through cardiac puncture from the left ventricle and centrifuged at 1620g for 20 min, 4°C; the serum obtained was used to determine the levels of triglycerides and total cholesterol (In vitro Diagnóstica), performed according to the manufacturer's instructions. Sample absorbance was read in an Epoch microplate reader (BioTekInstruments).

## 2.3 | Histopathological analyses

At euthanasia the animals were examined in order to identify palpable tumors and dissected in order to expose the lower genitourinary tract (bladder, seminal vesicles, and prostate lobes). The lower genitourinary tract was removed *en bloc* and then ventral prostate lobes were isolated, as well as the palpable tumors if present, and weighted. Ventral prostates and tumors were fixed in Boiun, for 24 h and processed for plastic polymer embedding (Paraplast; Merck). Histological sections were stained with Hematoxylin-Eosin and Picosirius-Hematoxylin for histopathological analyses. The microscopic images were obtained on a Zeiss-Jenaval microscope, AxioCam HRc digital camera coupled, and AxioVision Image analysis system (Carl-Zeiss).

The histopathological evaluation and other quantitative tissue analysis were carried out only for those prostate lobes that could be

properly isolated, since, in the massive tumors, there was a loss of tissue organization and variable pattern. The histopathological analysis was performed as described by Kido et al.,<sup>33</sup> with modifications. For each animal ( $n = 5/\text{group}$ ), 15 randomly microscopic fields were captured at x400 magnification and each one was divided into four quadrants. For each quadrant, the predominant morphological feature was classified as follows: (1) Normal epithelium; (2) LGPIN, represented by epithelial cell stratification; (3) HGPIN, marked by cell proliferation foci with papillary and cribriform pattern growth toward the glandular lumen; and (4) CIS, defined by small foci of stromal invasion or well-differentiated carcinoma, with multiple epithelial cancer cells in surrounding glandular stroma and preserved gland structures (Figure 1).

The evaluation of collagen fiber was performed in histological sections stained with Picosirius-Hematoxylin. The quantification of collagen fiber frequency was performed in 10 microscopic fields per animal ( $n = 5/\text{group}$ ) at x400 magnification, applying the multipoint system with 160 grid intersections.<sup>40</sup> The frequency was expressed by the number of positive grid intersections divided by the total number of grid intersections.

## 2.4 | Immunohistochemistry

Histological sections were subject to immunohistochemistry reactions for the detection of phospho-histone H3 (anti-PHH3; 1:75; rabbit polyclonal; #97015; Cell Signaling Biotechnology), AR (anti-AR; 1:75; rabbit polyclonal; sc-816; Santa Cruz Biotechnology), glucocorticoid receptor (GR) (anti-GR; 1:75; rabbit polyclonal; sc-1004; Santa Cruz Biotechnology), smooth muscle alpha actin (anti- $\alpha$ SMA; 1:100; mouse monoclonal; sc-32251; Santa Cruz Biotechnology), and cluster of differentiation 3 (anti-CD3; 1:100; rabbit monoclonal; ab16669; Abcam). Antigen retrieval was carried out by incubation of sections in a Tris-EDTA buffer (10 mM Trizma Base, 1 mM EDTA, 0.05% Tween 20, pH 9.0) or citrate buffer (10 mM, pH 6.0) for 45–60 min at 98°C. Sections were then incubated in  $H_2O_2$  3% during 15–30 min for endogenous peroxidase blockade. Nonspecific binding blockade was achieved by incubating the sections in a solution of BSA 3% for 1 h at room temperature. All primary antibodies were incubated overnight at 4°C and the antigen-antibody complexes were detected using peroxidase-conjugated polymer

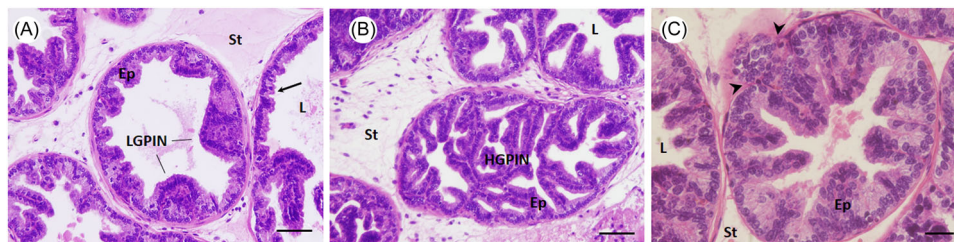


**FIGURE 1** Histological features of pathological lesions found in ventral prostate of TRAMP mice. (A) Normal epithelium (arrow) and low-grade PIN. (B) High-grade PIN. (C) Carcinoma in situ, arrowheads indicate the areas of basal membrane rupture. Stain, Hemataxylin-Eosin, scale bars: A, C, and D: 50 µm; B: 25 µm. Ep, epithelium; L, lumen; St, stroma; TRAMP, transgenic adenocarcinoma of the mouse prostate. [Color figure can be viewed at [wileyonlinelibrary.com](http://wileyonlinelibrary.com)]

(Novolink™ Max Polymer Detection System; Leica Biosystems) for androgen receptors (AR) or incubated with secondary biotin-conjugated antibody (dilution 1:200) and detected by avidin-biotin complex (ImmunoCruz® rabbit ABC Staining System; Santa Cruz Biotechnology) for the remaining antigens. Peroxidase activity was detected using diaminobenzidine (DAB; Leica Biosystems) as the chromogen. Harris hematoxylin was used for counter-staining and the negative controls were obtained by omitting the primary antibody.

Quantitative analyses were performed using Image-Pro Plus software (version 6.0; Media Cybernetics). The quantification of antigen reactivity was performed in 10 microscopic fields per animal ( $n = 5/\text{group}$ ) at  $\times 400$  magnification. In order to estimate the tissue expression of AR, GR, and  $\alpha\text{SMA}$ , the multipoint system with 160 grid intersections was applied.<sup>40</sup> Immunoreactivity was expressed by the number of the positive grid intersections divided by the total number of grid intersections. The result was expressed as relative frequency. In order to quantify PHH3 and CD3, the absolute number of positive cells in the 10 random microscopy fields of each animal were counted<sup>41</sup> and expressed as positive cells/field.

## 2.5 | Statistical analyses

Statistical analyses were performed using GraphPad Prism software (version 6.0.1). The data were evaluated by the Kolmogorov–Smirnov normality test and subjected to a comparison between the control- and ( $n-3$ ) PUFA-groups at the same age using an unpaired

$t$ -test (parametric data) or Mann–Whitney test (nonparametric data). Data were expressed as mean  $\pm$  standard deviation and  $p < 0.05$  was considered statistically significant.

## 3 | RESULTS

### 3.1 | ( $n-3$ ) PUFA improves serum cholesterol and triglycerides levels in TRAMP mice

Food intake and body weight gain did not vary between C12 and T12, although an increase of 1.3-fold in energy intake was observed (Figure 2A–C). Food and energy intake reduced in T20, when compared to C20, but body weight gain was unchanged (Figure 2A–C).

For both ages, ( $n-3$ ) PUFA lowered serum cholesterol (C8:  $33.5 \pm 5.5$ ; C12:  $34.8 \pm 4.7$ ; T12:  $23.5 \pm 2.31$ ; C20:  $43.3 \pm 7.2$ ; T20:  $29.64 \pm 4.38$  mg/dl) and triglycerides (C8:  $156 \pm 87.1$ ; C12:  $126 \pm 58.9$ ; T12:  $38 \pm 35$ ; C20:  $126 \pm 40.9$ ; T20:  $49 \pm 21.57$  mg/dl) (Figure 2D,E). ( $n-3$ ) PUFA also reduced fasting glucose in T20 compared to C20 by 1.2-fold (Figure 2F).

### 3.2 | ( $n-3$ ) PUFA delays tumor progression in TRAMP mice at early stage of disease

As expected for this transgenic model, no palpable tumors were detected for C8, C12, and T12, nor did the wet weight of the ventral

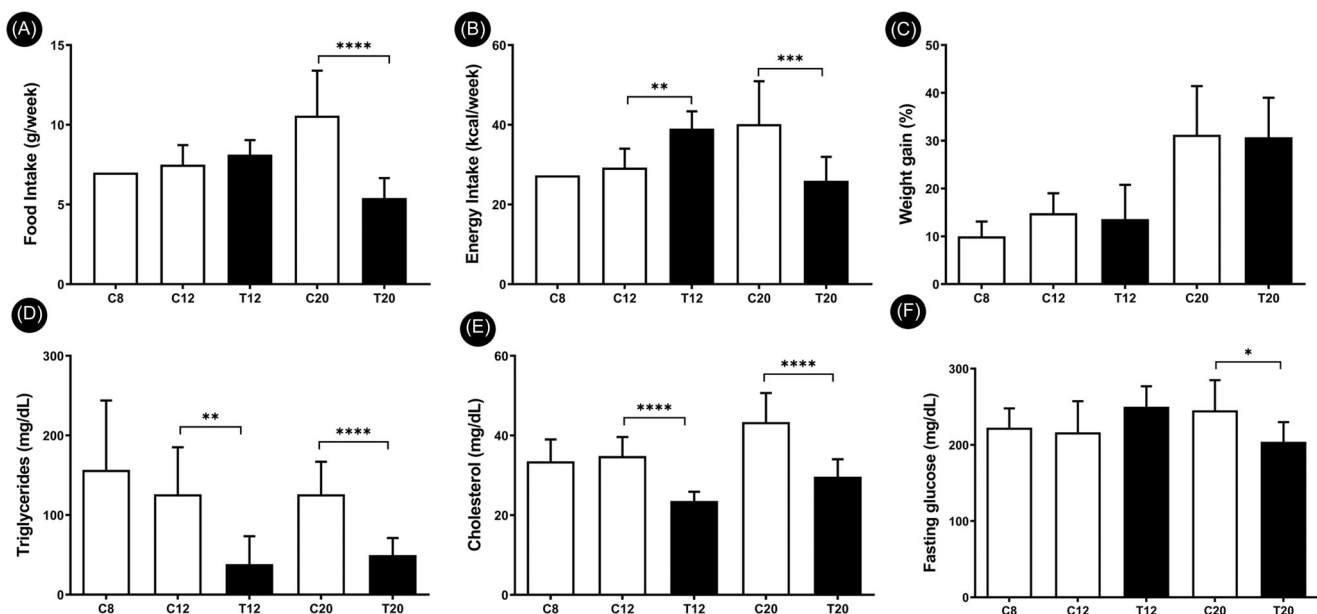


**FIGURE 2** Effect of DHA-enriched diet on biometric and metabolic features of TRAMP mice. (A) Food intake (g/week). (B) Energy intake (kcal/week). (C) Weight gain (%). (D) Serum triglycerides (mg/dl). (E) Serum cholesterol (mg/dl). (F) Fasting glucose (mg/dl). Statistics:  $t$ -test or Mann–Whitney. Bars indicated statistical difference between the experimental groups, \* $p < 0.05$ ; \*\* $p < 0.01$ ; \*\*\* $p < 0.001$ ; \*\*\*\* $p < 0.0001$ . Experimental groups: TRAMP mice 8-, 12-, or 20-week-old fed standard diet (C8, C12, and C20, respectively) or fed DHA-enriched diet for 4 (T12) or 8 weeks (T20). DHA, docosahexaenoic acid; TRAMP, transgenic adenocarcinoma of the mouse prostate.

prostate lobe change in these groups (C8:  $9.2 \pm 3.8$ ; C12:  $12.4 \pm 6.7$ ; T12:  $12.6 \pm 3.2$  mg). The histopathological analyses indicated that the ventral prostate of C8 already displayed many proliferative lesion foci (Figure 3), corresponding to a frequency of ~50% of LGPIN, ~14% of HGPIN, and ~3% of CIS (Figure 4). The ventral prostates of C12 exhibited 10% of normal epithelium, 26% of HGPIN, ~56% of LGPIN, and ~6% of CIS areas (Figures 3 and 4). The histopathological analyses indicated that the prostates of T12 exhibited a higher frequency of normal epithelium (~38%) and lower HGPIN (~7%) and (3%) CIS than C12 (Figures 3 and 4). Thus, (n-3) PUFA maintained prostate histology and the severity of pathological alterations in the T12 group at a level similar to that of the C8 group.

### 3.3 | (n-3) PUFA did not prevent primary tumor development, at an advanced stage of disease in the TRAMP mice

For both 20-week-old groups (C20, T20), half of the animals (5) developed a massive tumor, as a messy mass of accessory glands, and in this case neither the isolation of the ventral lobe nor an accurate histopathological analysis could be performed. At this age, histopathological analysis was therefore restricted to the animals (5) that did not develop a large tumor and whose prostatic lobes could be isolated properly. Neither the incidence (5 of 10 animals) nor the weight of tumors (C20:  $2.2 \pm 2.4$ ; T20:  $2.8 \pm 2.9$  g) varied between T20 and C20. A general histological analysis showed no difference between the tumors in the C20 and T20 groups (Figure 3P-U). For those animals that did not develop primary tumors whose ventral prostate could be properly isolated, the frequency of areas of normal epithelium in the gland was 8.8-fold higher in T20 when compared to C20 (C20: 5%; T20: 44%), the areas of HGPIN decreased 3.5-fold (C20: 32%; T20: 9%), and CIS was reduced to half (C20: 6%; T20: 3%) (Figures 3 and 4). Additionally, some sites of epithelial atrophy were observed in the gland of the T20 group (Figures 3 and 4).

### 3.4 | (n-3) PUFA mitigates stromal alterations in TRAMP

The glandular stroma of the 8-week-old TRAMP mice exhibited a normal phenotype marked by a collagen fiber arrangement around the prostatic acini, fibroblasts, and smooth muscle cells ( $\alpha$ SMA-positive). A similar aspect was observed in the glandular stroma of C12 but an accumulation of collagen fibers was detected particularly in the areas of proliferative disturbances (Figure 5). The prostate glandular stroma of T12 exhibited a lower stromal density than that of C12, attested by a decrease of 1.3-fold in collagen frequency and low reactivity for  $\alpha$ SMA ( $p = 0.0558$  vs. C12), resembling the features of C8 (Figure 5).

C20 animals exhibited a hypertrophic stroma with abundant collagen fibers around the prostatic acini and an increase in  $\alpha$ SMA-positive cells (C8: 6%; C12: 8%; C20: 13%) (Figure 5). The T20 group

displayed an improvement in the glandular stroma features with a reduction in collagen fibers by 1.4-fold and a lower frequency of  $\alpha$ SMA-positive cells in comparison to C20 (C20: 13%; T20: 7%) (Figure 5).

### 3.5 | (n-3) PUFA reduces cell proliferation, AR, and GR tissue expression

Lower proliferative rates were verified in the ventral prostate for T12 and T20 (C12:  $3.78 \pm 0.95$ ; T12:  $1.9 \pm 0.36$ ; C20:  $2.90 \pm 0.73$ ; T20:  $1.7 \pm 0.25$  cells per field) in comparison to same-age control groups (Figure 6).

(n-3) PUFA reduced AR-positive cells in the epithelium at early and advanced stages and stromal ones only in the latter (Figure 7). For both ages, (n-3) PUFA intake maintained AR-positive cells in the epithelial compartment at a level similar to that of C8 (C8:  $23 \pm 2.4$ ; T12:  $22 \pm 2.5$ ; T20:  $18 \pm 4.7$ ) (Figure 7). Regarding GR expression, GR-positive cells were lower in the epithelium and stroma of the gland in both groups fed with (n-3) PUFA (Figure 8).

### 3.6 | (n-3) PUFA decreases T-lymphocyte infiltration in the TRAMP mouse prostate

For all groups, the T-lymphocytes were observed in both epithelial and stromal compartments with a predominance of these cells in epithelial areas (Figure 9). The frequency of T-lymphocytes was reduced in the T20 group by 1.6-fold when compared with C20 (Figure 9).

## 4 | DISCUSSION

Preclinical and epidemiological studies support the idea that dietary interventions may delay the progression of established PCa and ameliorate the efficacy of cancer treatments.<sup>2,42</sup> These effects rely, at least in part, on the capacity of dietary interventions to modulate the metabolism of cancer cells and immune response,<sup>43</sup> both of which may potentially be influenced by (n-3) PUFA intake. Despite this, there is no consensus about the outcomes of (n-3) PUFAs on PCa.<sup>22-26</sup> In this scenario, controlled rodent studies in which hormonal, metabolic, and homeostatic context are also considered, as well as the interplay among several tissue components in the gland, may provide new information on this issue. Here we employed TRAMP mice, a model that replicates most parameters of human PCa progression,<sup>31,41,42</sup> to evaluate whether an (n-3) PUFA-enriched diet affects tumor progression at early and advanced stages of disease. The present data shows that dietary intervention at an early stage of PCa was able to lower the severity of the disease in the TRAMP ventral prostate. This delay was indicated by the preservation of healthy tissue and low frequency of HGPIN and CIS areas, resulting in a histopathological status of the gland very similar to the

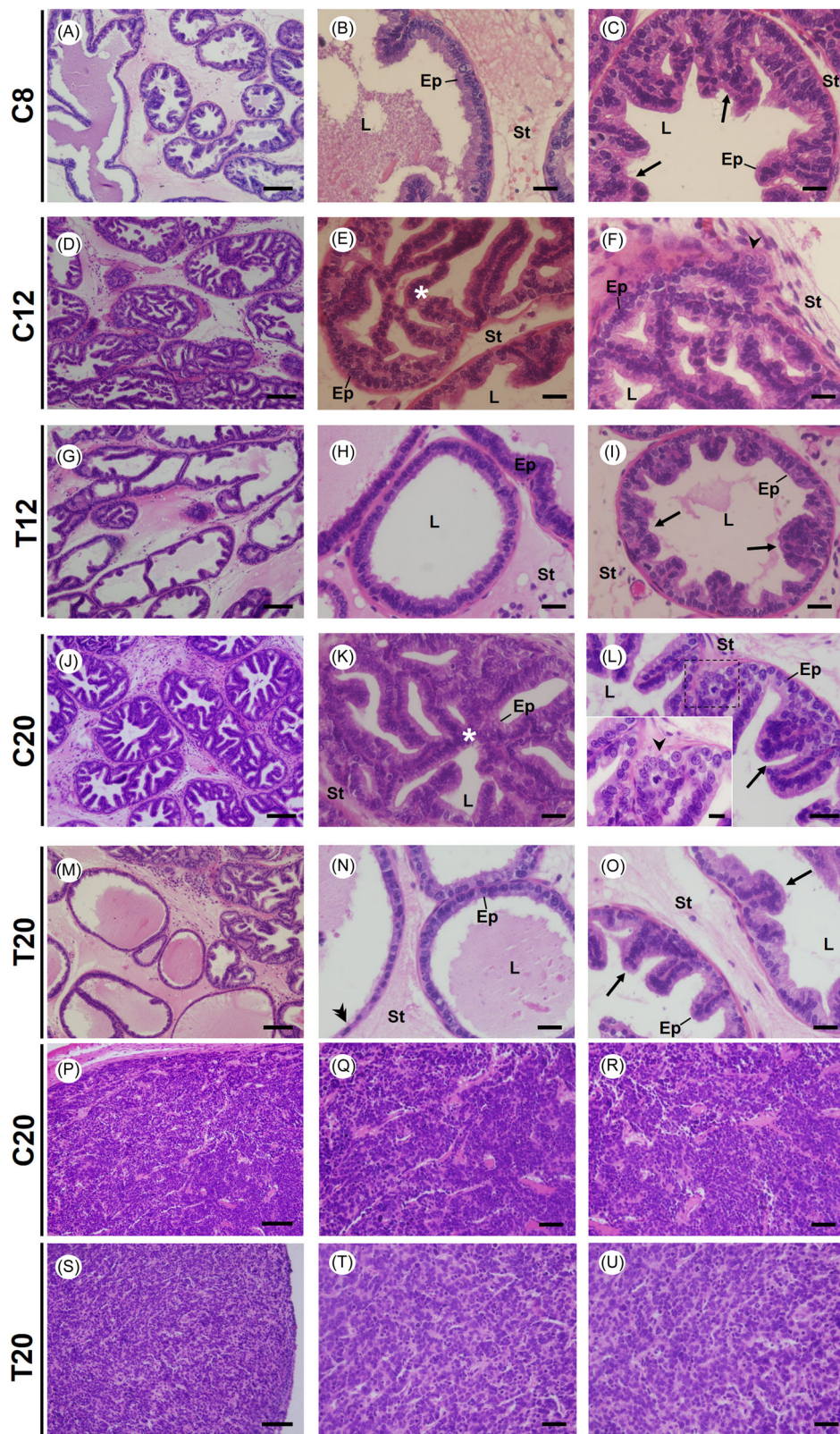


**FIGURE 3** Photomicrographs of the ventral prostate from the different experimental groups. Animals under dietary supplementation with DHA displayed a phenotype that resemble the initial stages of carcinogenesis (i.e., C8 group); however DHA intake did not prevent tumor development. Arrow: low-grade PIN; arrowhead: carcinoma in situ; asterisk: high-grade PIN, double arrowhead: atrophic epithelium. Stain: Hemataxylin-Eosin, scale bars: A, D, G, J, M: 100  $\mu$ m; P, S: 50  $\mu$ m, B, C, E, F, H, I, K, L, N, O, Q, R, T, U: 25  $\mu$ m, inset: 10  $\mu$ m. Experimental groups: TRAMP mice 8-, 12-, or 20-week-old fed standard diet (C8, C12, and C20, respectively) or fed DHA-enriched diet for 4 (T12) or 8 weeks (T20). DHA, docosahexaenoic acid; Ep, epithelium; L, lumen; St, stroma; TRAMP, transgenic adenocarcinoma of the mouse prostate. [Color figure can be viewed at [wileyonlinelibrary.com](http://wileyonlinelibrary.com)]

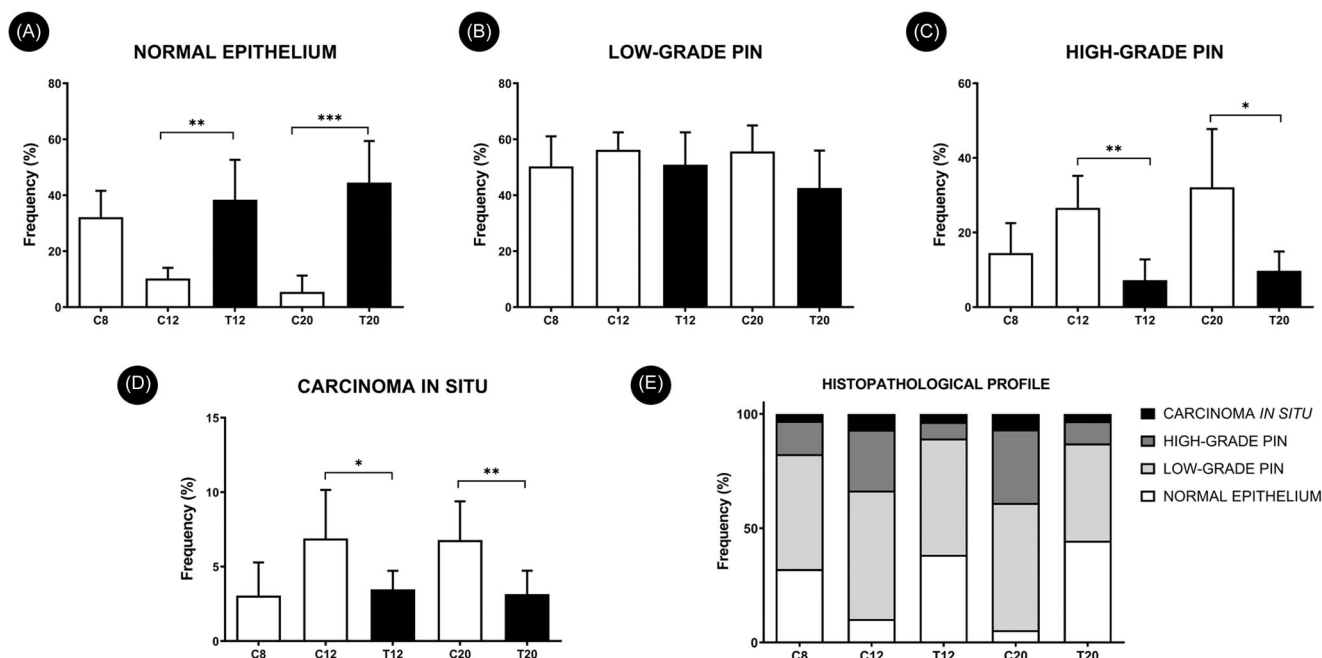


**FIGURE 4** Histopathological analysis. (A) Normal epithelium. (B) Low-grade PIN. (C) High-grade PIN. (D) Carcinoma in situ. (E) Histopathological profile. S Statistics: *t*-test or Mann-Whitney. Bars indicated statistical difference between the experimental groups, \**p* < 0.05; \*\**p* < 0.01; \*\*\**p* < 0.001; \*\*\*\**p* < 0.0001. Experimental groups: TRAMP mice 8-, 12-, or 20-week-old fed standard diet (C8, C12, and C20, respectively) or fed DHA-enriched diet for 4 (T12) or 8 weeks (T20). DHA, docosahexaenoic acid; TRAMP, transgenic adenocarcinoma of the mouse prostate.

initial stages of carcinogenesis (i.e., 8-week-old mice). Although the effects of different dietary or plant products have already been tested in TRAMP mice, few components were able to prevent the development of CIS in the ventral prostate, when provided in isolation,<sup>33,44,45</sup> which is reasonable considering the intensity of androgen signaling in this model. In this scenario, the maintenance of healthy areas and reductions in HGPIN and CIS suggest a delay in tumor progression and a protective role of (*n*-3) PUFA at initial phases of PCa (Table 1).

The delay in PCa progression induced by (*n*-3) PUFA in 12-week-old animals was related to decreased AR and GR expressions, preservation of lower cell proliferation rates and prevention of T-lymphocyte infiltrations in the gland. Saw et al.<sup>37</sup> showed that dietary intervention, for 10 weeks, with fish oil in the same proportion (10%) used herein led to a slight decrease in the incidence of palpable tumors and a reduction in tumor weight, carcinoma, and metastasis in TRAMP mice. However, no additional parameters of tissue gland response to (*n*-3) PUFA were examined by the present authors. Thus, to the best of our knowledge, this is the first study to assess in detail the effects of dietary (*n*-3) PUFA upon tumor progression in TRAMP mice.

Our results showed that one of mechanisms by which (*n*-3) PUFA intake delayed early-stage PCa progression in TRAMP mice is related to lower AR tissue expression. AR signaling regulates prostatic morphophysiology under normal conditions and its deregulation is a critical step in PCa pathogenesis.<sup>46</sup> During PCa progression, the expression of AR gradually increases and correlates

with disease severity in both human and TRAMP models.<sup>44,47</sup> It has been reported that PUFA DHA caused no alteration in the mRNA expression levels of the AR in premalignant (PNTA1) and tumor 22rv1, LNCaP, and PC3 prostate cells.<sup>11,48</sup> For hormone-sensitive LNCaP cells<sup>11</sup> and PTEN<sup>-/-</sup> mice,<sup>49</sup> the effect of DHA on lowering AR content was due to a stimulation of its proteasomal degradation. In vivo studies also showed that DHA/EPA intake reduces AR content in C3(1)Tag<sup>50</sup> and PTEN<sup>-/-</sup> mice.<sup>49</sup> The present data therefore confirm previous in vitro results, demonstrating that dietary (*n*-3) PUFAs is able to reduce androgenic signaling in the prostate and delaying tumor progression at early stages in TRAMP, suggesting a protective action in this phase of PCa. Niu et al.<sup>51</sup> have compared the differential roles of AR in stromal and epithelial cells in prostate carcinogenesis of TRAMP using a knockout model of AR in both the prostate epithelium and stroma (indARKO-TRAMP) or in the epithelium alone (pes-ARKO-TRAMP). The present authors demonstrated that AR knockout in both epithelium and stroma decreased tumor growth by lowering cell proliferation and tumor stromal invasiveness, whereas the selective AR knockout in the epithelium resulted in larger primary prostate tumors with higher proliferation rates. Thus, it was concluded that stromal AR might play a more dominant role than epithelial AR to promote primary tumor proliferation in the early stages of PCa. In this context, the effects of (*n*-3) PUFAs on reducing stromal expression of AR is an interesting mechanism by which (*n*-3) PUFA could impair PCa progression.

In the present research we have observed that dietary (*n*-3) PUFA reduced GR tissue expression in both epithelium and gland

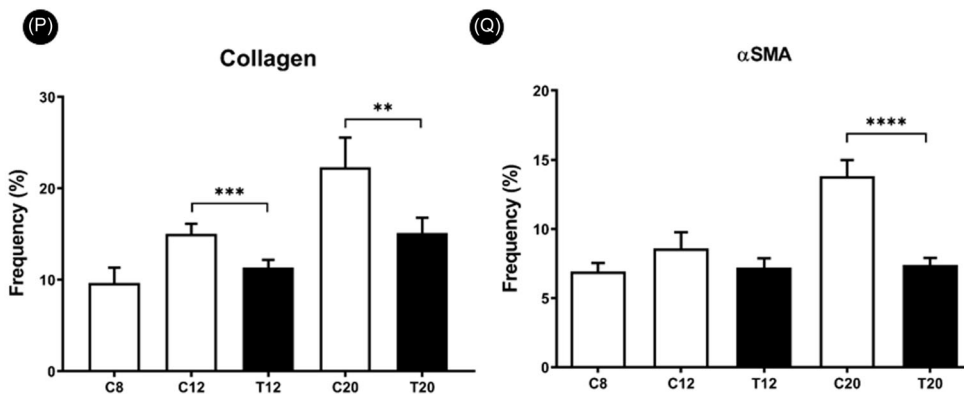
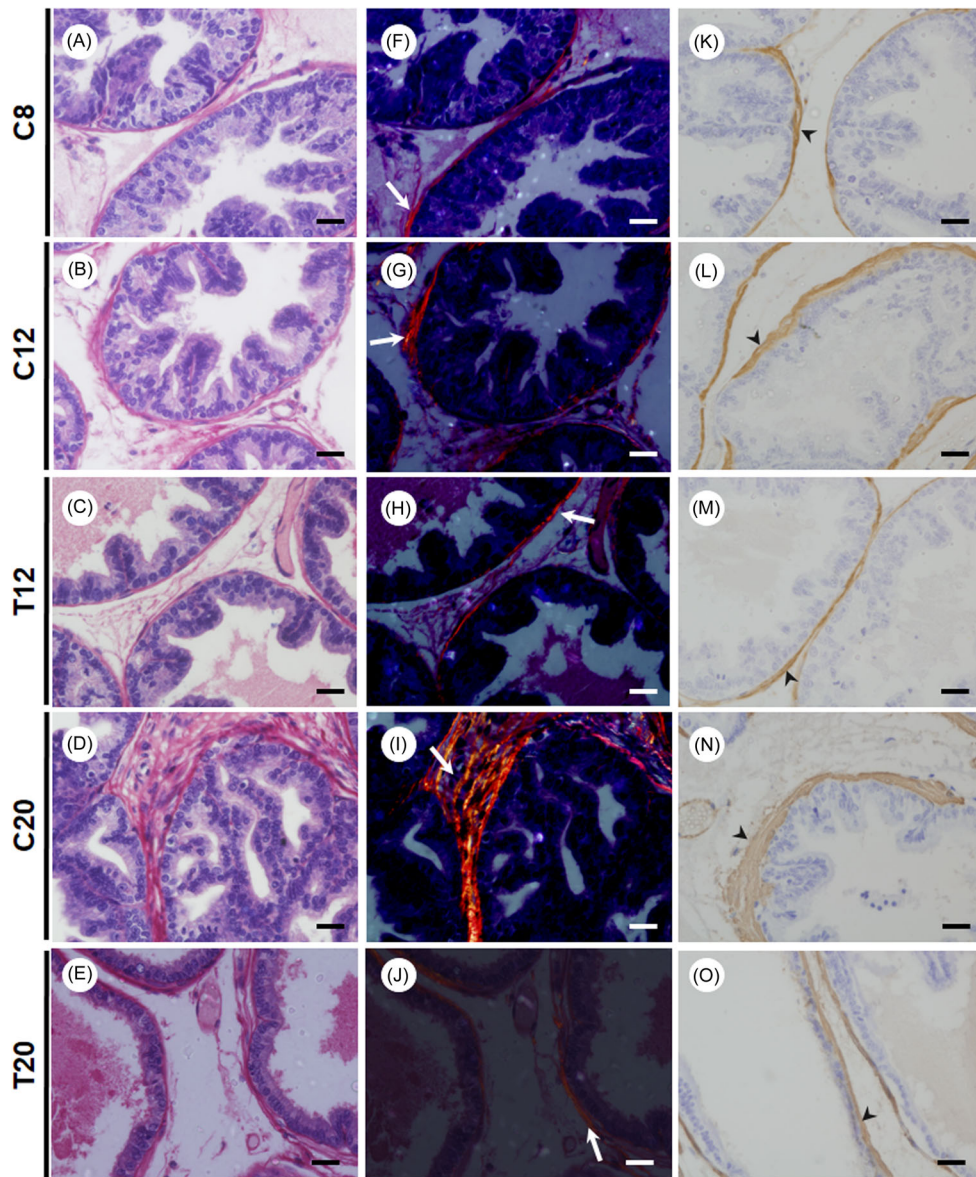


**FIGURE 5** Stromal architecture among the experimental groups. Arrows indicate collagen fibers and arrowheads immunoreactivity for  $\alpha$ SMA. (A–E) Picosirius-Hematoxylin. (F–J) Picosirius-Hematoxylin under polarized light. (K–O) Immunohistochemistry for  $\alpha$ SMA. (P) Quantification of collagen frequency. (Q) Quantification of  $\alpha$ SMA expression. Statistics: *t*-test. Bars indicated statistical difference between the experimental groups, \* $p < 0.05$ ; \*\* $p < 0.01$ ; \*\*\* $p < 0.001$ ; \*\*\*\* $p < 0.0001$ . Experimental groups: TRAMP mice 8-, 12-, or 20-week-old fed standard diet (C8, C12, and C20, respectively) or fed DHA-enriched diet for 4 (T12) or 8 weeks (T20). Scale bars: 25  $\mu$ m.  $\alpha$ SMA, alpha smooth muscle actin; DHA, docosahexaenoic acid; TRAMP, transgenic adenocarcinoma of the mouse prostate. [Color figure can be viewed at [wileyonlinelibrary.com](http://wileyonlinelibrary.com)]

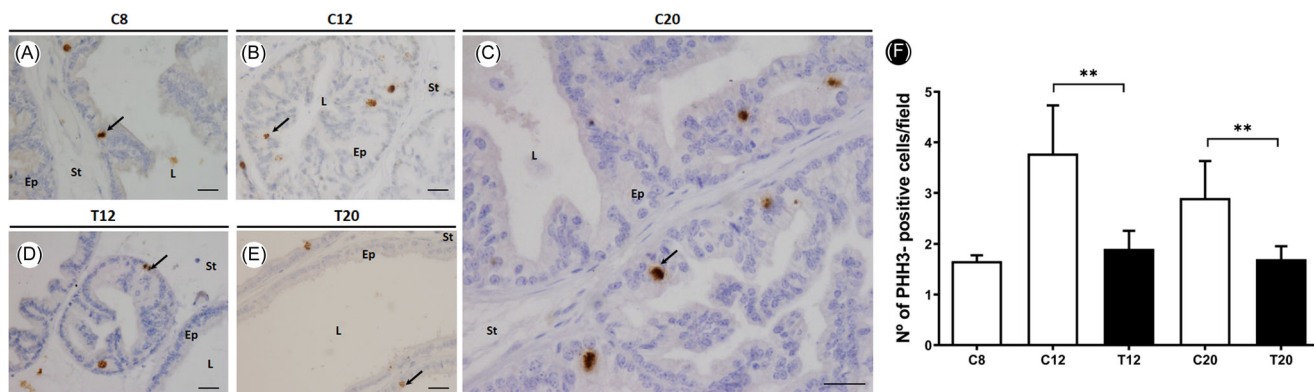


**FIGURE 6** Detection of proliferative cells in the ventral prostate of the experimental groups. (A–E) Immunohistochemistry for PHH3, arrows indicate positive cells. (F) Quantification of PHH3-positive cells. Statistics: *t*-test. Bars indicated statistical difference between the experimental groups, \**p* < 0.05; \*\**p* < 0.01; \*\*\**p* < 0.001; \*\*\*\**p* < 0.0001. Experimental groups: TRAMP mice 8-, 12-, or 20-week-old fed standard diet (C8, C12, and C20, respectively) or fed DHA-enriched diet for 4 (T12) or 8 weeks (T20). Scale bars: 25  $\mu$ m. DHA, docosahexaenoic acid; Ep, epithelium; L, lumen; PHH3, phospho-histone H3; St, stroma; TRAMP, transgenic adenocarcinoma of the mouse prostate. [Color figure can be viewed at [wileyonlinelibrary.com](http://wileyonlinelibrary.com)]

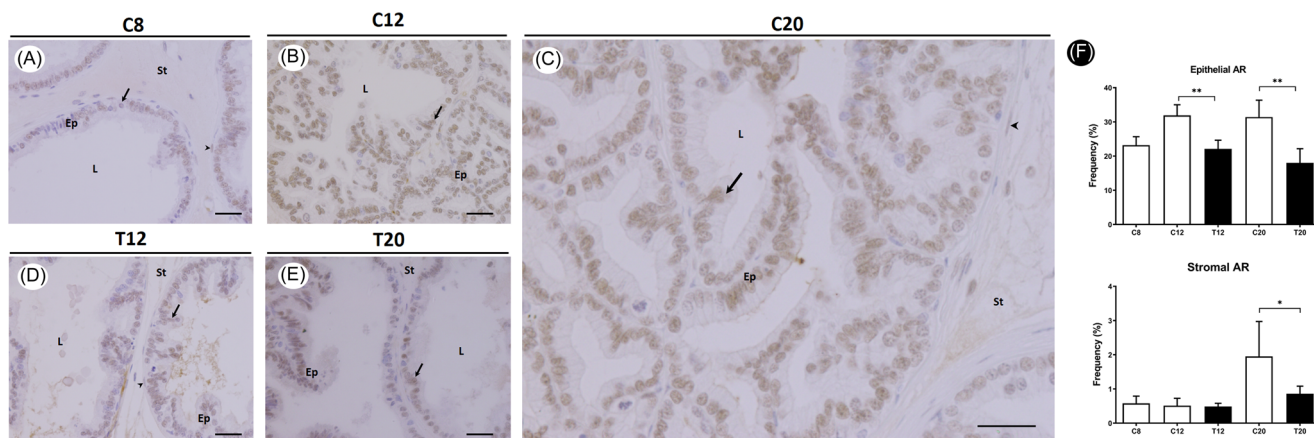


**FIGURE 7** Androgen receptor (AR) tissue expression in the experimental groups. (A–E) Immunohistochemistry for AR. (F) Quantification of AR immunoreactivity. Arrows and arrowheads indicate positive cells in the epithelial and stromal compartments. Statistics: *t*-test. Bars indicated statistical difference between the experimental groups, \**p* < 0.05; \*\**p* < 0.01; \*\*\**p* < 0.001; \*\*\*\**p* < 0.0001. Experimental groups: TRAMP mice 8-, 12-, or 20-week-old fed standard diet (C8, C12, and C20, respectively) or fed DHA-enriched diet for 4 (T12) or 8 weeks (T20). Scale bars: 25  $\mu$ m. DHA, docosahexaenoic acid; Ep, epithelium; L, lumen; St, stroma; TRAMP, transgenic adenocarcinoma of the mouse prostate. [Color figure can be viewed at [wileyonlinelibrary.com](http://wileyonlinelibrary.com)]

stroma at early stages of PCa in TRAMP mice. The capacity of PUFA DHA to reduce the expression of GR has been previously observed by Champeil-Potokar et al.<sup>52</sup> in cultured rat astrocytes, resulting in an anti-corticosterone effect and modulation of astrocyte phenotype. However, to the best of our knowledge, this is the first report showing an action of dietary (*n*-3) PUFA on tissue expression of this receptor in the prostate. As the activation of GR has a mitogenic effect on the rodent prostate,<sup>53,54</sup> low GR expression may also contribute to reduced cell proliferation levels and a delay in PCa progression by (*n*-3) PUFA. GR is a member of the nuclear receptor superfamily, which shares a conserved DNA-binding domain with the other members of the steroid subgroup,<sup>55</sup> and a possible cross

communication between nuclear receptor signaling is crucial for prostatic carcinogenesis. It should be noted that the role of GR signaling in the prostate is complex, as corticosterone demonstrates an ambivalent contribution in PCa and, in the context of functional AR signaling, GR activation might slow down cell proliferation, whereas, in the context of AR blockage, it might reactivate AR signaling.<sup>56</sup> Nevertheless, although AR signaling has a major role in PCa onset and progression, it is known that individuals receiving androgen deprivation therapy eventually develop a resistance phenotype known as castration-resistant prostate cancer (CRPC), leading to an imbalance in the expression of many nuclear receptors, among them GR.<sup>56,57</sup> Anti-androgen treatments of prostate cells lead

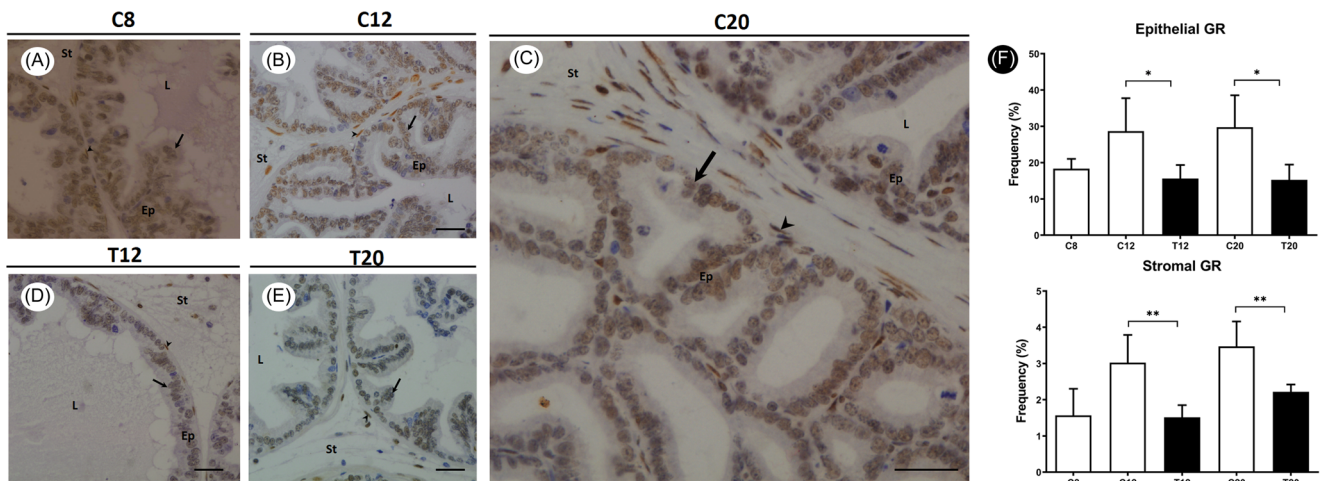


**FIGURE 8** Glucocorticoid receptor (GR) tissue expression in the experimental groups. (A–E) Immunohistochemistry for GR. (F) Quantification of GR immunoreactivity. Arrows and arrowheads indicate positive cells in the epithelial and stromal compartments, respectively. Statistics: *t*-test. Bars indicated statistical difference between the experimental groups, \**p* < 0.05; \*\**p* < 0.01; \*\*\**p* < 0.001; \*\*\*\**p* < 0.0001. Experimental groups: TRAMP mice 8-, 12-, or 20-week-old fed standard diet (C8, C12, and C20, respectively) or fed DHA-enriched diet for 4 (T12) or 8 weeks (T20). Scale bars: 25  $\mu$ m. DHA, docosahexaenoic acid; Ep, epithelium; L, lumen; St, stroma; TRAMP, transgenic adenocarcinoma of the mouse prostate. [Color figure can be viewed at [wileyonlinelibrary.com](http://wileyonlinelibrary.com)]

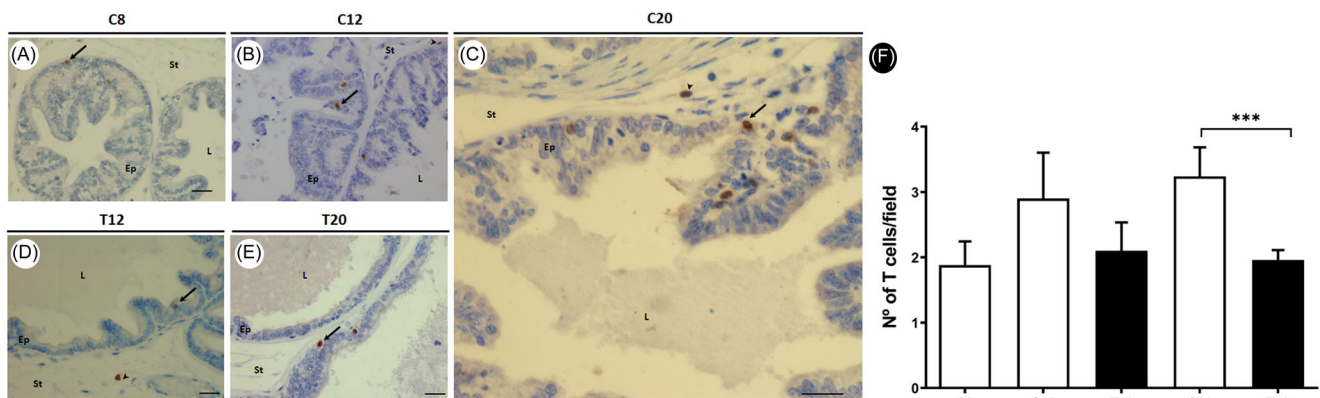


**FIGURE 9** Effect of fish oil intake on T-lymphocyte infiltrate. (A–E) Immunohistochemistry for CD3, CD3-positive cells appear in brown. (F) Quantification of T-lymphocyte in ventral prostate of the experimental groups. Note the higher number of T-lymphocytes in PIN foci (B and C). Statistics: *t*-test. Bars indicated statistical difference between the experimental groups, \**p* < 0.05; \*\**p* < 0.01; \*\*\**p* < 0.001; \*\*\*\**p* < 0.0001. Experimental groups: TRAMP mice 8-, 12-, or 20-week-old fed standard diet (C8, C12, and C20, respectively) or fed DHA-enriched diet for 4 (T12) or 8 weeks (T20). Scale bars: 25  $\mu$ m. CD3, cluster of differentiation 3; DHA, docosahexaenoic acid; Ep, epithelium; L, lumen; St, stroma; TRAMP, transgenic adenocarcinoma of the mouse prostate. [Color figure can be viewed at [wileyonlinelibrary.com](http://wileyonlinelibrary.com)]

to an overexpression of GR, suggesting the existence of an AR-mediated negative feedback in GR expression.<sup>58</sup> In this case, GR overexpression is a critical event for cell survival since it promotes the bypass of the androgenic blockade, and recuperates the expression of several androgen-regulated genes.<sup>58</sup> Additionally, castration-resistant cells show a loss of 11 $\beta$ -hydroxysteroid dehydrogenase II (11 $\beta$ -HSDII) expression, which results in overstimulation of GR through the maintenance of glucocorticoid levels in their active form.<sup>59</sup> Collectively, these findings highlight an important role of GR in paracrine signaling in the prostatic microenvironment, and suggest that the increasing stromal expression of this receptor might be an important event in disease progression to an aggressive

stage and the acquiring of a hormone-refractory phenotype. In this context, an (*n*–3) PUFA-induced decrease of GR mitigated the progression of the initial phases of CaP via a reduction in cell proliferation and the preservation of epithelium-stroma interactions in the gland.

The tumor microenvironment has a profound influence on the development and progression of neoplastic lesions.<sup>60</sup> The set of alterations in extracellular matrix components, diffusible growth factors and cytokines, designed as reactive stroma, supports cell proliferation, induces a myofibroblast phenotype and favors metastasis.<sup>61</sup> Stromal hypertrophy, characterized by an increase in  $\alpha$ SMA and collagen expression, is an event already reported in the TRAMP

**TABLE 1** Composition of the diets offered to the experimental groups

Ingredients (g/1-00.48 g)	Standard diet	Omega-3 diet
Casein	20	20
Corn starch	52.950	42.950
Sucrose	10	10
Soybean oil	7	7
Fish oil	-	10
Cellulose	5	5
AIN-93G mineral mix	3.5	3.5
AIN-93G vitamin mix	1	1
Choline bitartrate	0.25	0.25
L-cystine	0.3	0.3
Butylated hydroxytoluene	0.476	0.476
Total	100.476	100.476
Energy amount (kcal/g)	3.9	4.8

model that highlights a positive correlation between these stromal features and disease severity.<sup>45</sup> Our data indicate that (n-3) PUFA improved the stroma microenvironment in the prostate, preserving the microscopic features of prostate stroma, the amount and distribution of collagen fibers, and the tissue expression of  $\alpha$ SMA. The downregulation in  $\alpha$ SMA suggests that (n-3) PUFA impairs myofibroblast formation, and these findings are in accordance with previous reports demonstrating that DHA downregulated  $\alpha$ SMA expression in a chemically induced model of HPB in rats,<sup>62</sup> reduced the activation of fibroblasts into myofibroblasts,<sup>63</sup> and decreased fibrogenesis in mice under hepatic-induced fibrosis.<sup>64</sup> DHA also decreased the expression of MMP-9 and invasion induced by 12-O-tetradecanoylphorbol-13-acetate (TPA) in the MCF-7 breast cancer cell line through modulation of the MAPK signaling pathway and PPAR- $\gamma$ /NF- $\kappa$ B activity.<sup>65</sup> Thus, our results point to stromal environment preservation as another way by which (n-3) PUFAs delay tumor progression.

Recent approaches in PCa treatment are targeting the inflammatory process to delay the evolution of the disease.<sup>33,66</sup> Indeed, (n-3) PUFA has an impressive anti-inflammatory property, downregulating the NF- $\kappa$ B transcription factor pathway.<sup>20</sup> The present data showing a reduction in CD3<sup>+</sup> lymphocytes may suggest an anti-inflammatory action of dietary (n-3) PUFA on the prostate. CD3<sup>+</sup> lymphocyte reduction is coherent with an environment high in (n-3) PUFA, since it has been reported that both DHA and EPA impaired lipid raft composition through a reduction in sphingomyelin content and the displacement of PKC in the membrane rafts,<sup>67</sup> downregulating MPK signaling,<sup>68</sup> and impacting T-cell migration.<sup>69</sup> Previous studies reported increased CD3<sup>+</sup> cell infiltrates in human PCa samples<sup>70,71</sup> and mouse models,<sup>72</sup> correlating with PTEN loss and ERG fusion and a worse prognosis of PCa.<sup>71,73</sup> The reduction in CD3<sup>+</sup> might

therefore be related to delaying the progression of the disease. However, the present data does not allow us to discern which subtype of T-cell was affected by (n-3) PUFA intake, and we cannot exclude the possibility that (n-3) PUFA could be downregulating CD4<sup>+</sup> and CD4<sup>+</sup>/FOXP3<sup>+</sup>, both related to tumor onset and progression.<sup>74</sup> The overall reduction in T-cell population in the TRAMP mice prostate highlights the need for additional studies of the effects of (n-3) PUFA on T-cell subtypes and the lymphocyte population in PCa that will help to clarify the role of these cells in disease onset and progression.

Decreases of triglycerides and cholesterol serum levels were the most significant metabolic outcomes of (n-3) PUFA observed here. Indeed, fish oil supplementation has been used for cardiovascular disease management due to its capacity to improve lipid metabolism.<sup>75</sup> Furthermore, it should be noted that the dietary intake in the present study is closely related to the 0.2–5 g of DHA + EPA/day recommended for cardiovascular protection.<sup>76</sup> High levels of serum triglycerides and cholesterol have already been associated with the increasing risk of PCa development and recurrence.<sup>77,78</sup> Hypertriglyceridemia can induce insulin resistance and promote oxidative stress, both risk factors for PCa development.<sup>79,80</sup> Recently, it has been reported that serum cholesterol levels correlate positively with epithelial proliferation and with the intraprostatic levels of androgen in the PTEN<sup>-/-</sup> mice.<sup>81</sup> In the present study we detected an increase in cholesterol levels in TRAMP mice at 20-week age, which suggests an alteration in cholesterol metabolism during tumor progression in this model. The lowering effect of (n-3) PUFA on serum cholesterol and triglycerides levels reinforces the notion that a modulation of lipid metabolism might be an important target to delay PCa progression. Previous reports have shown that this effect in reducing serum cholesterol and triglycerides levels by (n-3) PUFA may be due to the downregulation of the hepatic expression of the fatty acid synthase and HMG-CoA reductase (3-hydroxy-3-methylglutaryl-CoA reductase), which are key enzymes for triglycerides and cholesterol de novo synthesis.<sup>82,83</sup>

The response to (n-3) PUFA detected in the 20-week age group was intriguing because, for half of the animals, PUFAs neither prevented primary tumor development nor affected the tumor weight, but, for the other half, it clearly mitigated the severity of the disease. In the latter case, gland structure was preserved and histology remained similar to that of 8-week age animals, with regard to the proportion of healthy areas, HGPIN, and CIS. Moreover, for these animals, (n-3) PUFA-intake led to a prostate response similar to that found in early stages of PCa, reducing AR and GR tissue expression, decreasing cell proliferation, and T-lymphocyte infiltrations, and preserving the stromal microenvironment in the gland. Greenberg et al.,<sup>27</sup> who developed an improved TRAMP model, have shown that ablation of androgen signaling due to castration significantly decreases tumor burden but does not affect the overall progression to an undifferentiated phenotype and metastasis. According to these authors, these results reflect the heterogeneity of PCa in this model regarding androgen dependency, in addition to the presence of both androgen-dependent and -independent cells in

primary tumors. The different response to (*n*-3) PUFA found in subsets of 20-week age mice may reflect such heterogeneity. Indeed, our *in vivo* data matches with *in vitro* results.<sup>48</sup> Human epithelial premalignant prostate cells PNT1A (AR-FL+; AR-Vs-; PTEN+) are more responsive to DHA regarding the deregulation of metabolism and androgen-related genes compared to 22rv1 (AR-FL+; AR-Vs+; PTEN0+) and PC3 (AR-FL-; PTEN-).<sup>48</sup> Recent results obtained in our laboratory also show that the response to PUFA DHA involves a differential lipid metabolism in advanced tumor cells, since 22rv1 has been described as increasing DHA oxidation using it as an energy source (data not shown) and retro-converting it into EPA. In addition, these cell lines also increased lipogenesis from glutamine, a known mechanism of resistance in CRPC (data not shown). On the other hand, premalign PNT1A did not oxidize DHA at higher rates but accumulated it instead, increasing its susceptibility to oxidative damage. This also resulted in remarkable mitochondrial impairment. Distinct metabolic alteration also reflected on the cell cycle which, in both AR-positive cells described, had a decreased S-phase and triggered cell death, whereas, in AR-negative cells, it arrested in G2/M.<sup>48</sup> The present results, despite their focus on CRPC cells, show that, at advanced stages, *n*-3 PUFAs have distinct effects on PCa cell growth, which may support the heterogeneity that was observed. Our results also indicate the need for further *in vivo* investigation to elucidate the efficacy of *n*-3 PUFAs in advanced stages of PCa progression.

## 5 | CONCLUSION

Our data indicate that (*n*-3) PUFAs delay tumor progression in the TRAMP model, in the early stages of disease. This protective action is associated with a decrease in cell proliferation, reduction of AR and GR tissue expression, lower T-lymphocyte infiltrate, and features of metabolic improvement. Our findings also reinforce the requirement of additional studies concerning the action of PUFA in more advanced stages of PCa

### ACKNOWLEDGMENT

This work was supported by São Paulo State Research Foundation—FAPESP (Grant to Rejane M. Góes: 2018/21891-4; Alana D. T. da Silva: 2019/15109-4), by National Council of Technological and Scientific Development—CNPq (Grants to Gustavo M. Amaro: 308367/2014-6; Rejane M. Góes 311635/2017) and by Coordination for the Improvement of Higher Education Personnel—CAPES (Grants to Alana D. T. da Silva and Guilherme H. Tamarindo, Finance Code 001).

### CONFLICT OF INTEREST

The authors declare no conflict of interest.

### DATA AVAILABILITY STATEMENT

The data that support the findings of this study are openly available in Repositório Institucional UNESP at <https://repositorio.unesp.br/handle/11449/192715>

### ORCID

Sebastião R. Taboga  <http://orcid.org/0000-0002-0970-4288>

Valéria Helena Alves Cagnon  <http://orcid.org/0000-0001-5331-7376>

Rejane M. Góes  <http://orcid.org/0000-0002-3622-460X>

### REFERENCES

1. Siegel RL, Miller KD, Jemal A. Cancer statistics, 2020. *CA Cancer J Clin.* 2020;70:7-30.
2. Mokbel K, Wazir U, Mokbel K. Chemoprevention of prostate cancer by natural agents: evidence from molecular and epidemiological studies. *Anticancer Res.* 2019;39:5231-5259.
3. Emilio S, Luigi V, Riccardo B, Carlo G. Lifestyle in urology: cancer. *Urol J.* 2019;86:105-114.
4. Ravasco P. Nutrition in cancer patients. *J Clin Med.* 2019;8:1-13.
5. Ferrucci D, Silva SP, Rocha A, et al. Dietary fatty acid quality affects systemic parameters and promotes prostatitis and pre-neoplastic lesions. *Sci Rep.* 2019;9:1-15.
6. Hayashi T, Fujita K, Nojima S, et al. High-fat diet-induced inflammation accelerates prostate cancer growth via IL6 signaling. *Clin Cancer Res.* 2018;24:1-11.
7. Kelavkar UP, Hutzley J, Dhir R, Kim P, Allen KGD, McHugh K. Prostate tumor growth and recurrence can be modulated by the  $\omega$ -6: $\omega$ -3 ratio in diet: athymic mouse xenograft model simulating radical prostatectomy. *Neoplasia.* 2006;8(2):112-124.
8. Ribeiro DL, Pinto ME, Rafacho A, et al. High-fat diet obesity associated with insulin resistance increases cell proliferation, estrogen receptor, and PI3K proteins in rat ventral prostate. *J Androl.* 2012;33:854-865.
9. Ribeiro DL, Pinto ME, Maeda SY, Taboga SR, Góes RM. High fat-induced obesity associated with insulin-resistance increases FGF-2 content and causes stromal hyperplasia in rat ventral prostate. *Cell Tissue Res.* 2012;349:577-588.
10. Cho HJ, Kwon GT, Park H, et al. A high-fat diet containing lard accelerates prostate cancer progression and reduces survival rate in mice: possible contribution of adipose tissue-derived cytokines. *Nutrients.* 2015;7:2539-2561.
11. Hu Z, Qi H, Zhang R, et al. Docosahexaenoic acid inhibits the growth of hormone-dependent prostate cancer cells by promoting the degradation of the androgen receptor. *Mol Med Rep.* 2015;12(3):3769-3774.
12. Kobayashi N, Barnard RJ, Henning SM, et al. Effect of altering dietary  $\omega$ -6/ $\omega$ -3 fatty acid ratios on prostate cancer membrane composition, cyclooxygenase-2, and prostaglandin E2. *Clin Cancer Res.* 2006;12:4662-4670.
13. Salem N, Eggersdorfer M. Is the world supply of omega-3 fatty acids adequate for optimal human nutrition? *Curr Opin Clin Nutr Metab Care.* 2015;18:147-154.
14. Elagizi A, Lavie CJ, Marshall K, Dinicolantonio JJ, Keefe JHO, Milani RV. Progress in cardiovascular diseases omega-3 polyunsaturated fatty acids and cardiovascular health: a comprehensive review. *Prog Cardiovasc Dis.* 2018;61:1-10.
15. Hu Y, Sun H, Owens RT, et al. Syndecan-1-dependent suppression of PDK1/Akt/bad signaling by docosahexaenoic acid induces apoptosis in prostate cancer. *Neoplasia.* 2010;12:826-836.
16. Sun Y, Jia X, Hou L, Liu X, Gao Q. Involvement of apoptotic pathways in docosahexaenoic acid-induced benefit in prostate cancer: pathway-focused gene expression analysis using RT2 profile PCR array system. *Lipids Health Dis.* 2017;16:1-8.
17. Cavazos DA, Price RS, Apte SS, Linda A. Docosahexaenoic acid selectively induces human prostate cancer cell sensitivity to oxidative stress through modulation of NF-kB. *Prostate.* 2011;1428:1420-1428.

18. Tamarindo GH, Ribeiro DL, Gobbo MG, et al. Melatonin and docosahexaenoic acid decrease proliferation of PNT1A prostate benign cells via modulation of mitochondrial bioenergetics and ROS production. *Oxid Med Cell Longev*. 2019;2019:1-15.
19. Liang P, Henning SM, Guan J, et al. Effect of dietary omega-3 fatty acids on castrate-resistant prostate cancer and tumor-associated macrophages. *Prostate Cancer Prostatic Dis*. 2019;23:127-135.
20. Liang P, Henning SM, Schokrpur S, et al. Effect of dietary omega-3 fatty acids on tumor-associated macrophages and prostate cancer progression. *Prostate*. 2016;76:1293-1302.
21. Lloyd JC, Masko EM, Wu C, et al. Fish oil slows prostate cancer xenograft growth relative to other dietary fats and is associated with decreased mitochondrial and insulin pathway gene expression. *Prostate Cancer Prostatic Dis*. 2013;16:285-291.
22. Leitzmann MF, Stampfer MJ, Michaud DS, et al. Dietary intake of n-3 and n-6 fatty acids and the risk of prostate. *Am J Clin Nutr*. 2004;80:204-216.
23. Lovegrove C, Ahmed K, Challacombe B, Khan MS, Popert R, Dasgupta P. Systematic review of prostate cancer risk and association with consumption of fish and fish-oils: analysis of 495,321 participants. *Int J Clin Pract*. 2015;69:87-105.
24. Zhao Z, Reinstatler L, Klaassen Z, et al. The association of fatty acid levels and gleason grade among men undergoing radical prostatectomy. *PLoS One*. 2016;11:1-9.
25. Brasky TM, Till C, White E, et al. Serum phospholipid fatty acids and prostate cancer risk: results from the prostate cancer prevention trial. *Am J Epidemiol*. 2011;173:1429-1439.
26. Sorongon-Legaspi MK, Chua M, Sio MC, Morales M. Blood level omega-3 fatty acids as risk determinant molecular biomarker for prostate cancer. *Database Abstr Rev Eff*. 2013;2013:1-15.
27. Gingrich JR, Barrios RJ, Kattan MW, Nahm HS, Finegold MJ, Greenberg NM. Androgen-independent prostate cancer progression in the TRAMP model. *Cancer Res*. 1997;57:4687-4691.
28. Bono AV, Montironi R, Pannellini T, et al. Effects of castration on the development of prostate adenocarcinoma from its precursor HGPIN and on the occurrence of androgen-independent, poorly differentiated carcinoma in TRAMP mice. *Prostate Cancer Prostatic Dis*. 2008;11:377-383.
29. Han G, Foster BA, Mistry S, et al. Hormone status selects for spontaneous somatic androgen receptor variants that demonstrate specific ligand and cofactor dependent activities in autochthonous prostate cancer. *J Biol Chem*. 2001;276:11204-11213.
30. Kido LA, Almeida CDe, Roberto M, Jr., M, Helena V, Cagnon, A. Transgenic adenocarcinoma of the mouse prostate (TRAMP) model: a good alternative to study PCA progression and chemoprevention approaches. *Life Sci*. 2019;217:141-147.
31. Shukla S, MacLennan GT, Marengo SR, Resnick MI, Gupta S. Constitutive activation of PI3K-Akt and NF- $\kappa$ B during prostate cancer progression in autochthonous transgenic mouse model. *Prostate*. 2005;64:224-239.
32. Pflug BR, Pecher SM, Brink AW, Nelson JB, Foster BA. Increased fatty acid synthase expression and activity during progression of prostate cancer in the TRAMP model. *Prostate*. 2003;57:245-254.
33. Kido LA, Montico F, Sauce R, et al. Anti-inflammatory therapies in TRAMP mice: delay in PCA progression. *Endocr Relat Cancer*. 2016;23:235-250.
34. Greenberg NM, Demayo F, Finegold MJ, et al. Prostate cancer in a transgenic mouse. *Med Sci*. 1995;92:3439-3443.
35. Kaplan-Lefko PJ, Chen TM, Ittmann MM, et al. Pathobiology of autochthonous prostate cancer in a pre-clinical transgenic mouse model. *Prostate*. 2003;55(3):219-237.
36. Reeves PG, Nielsen FH, Fahey GC. AIN-93 purified diets for laboratory rodents: final report of the American Institute of Nutrition ad hoc writing committee on the reformulation of the AIN-76A rodent diet. *J Nutr*. 1993;123:1939-1951.
37. Saw CLL, Wu TY, Paredes-Gonzalez X, Khor TO, Pung D, Tony Kong AN. Pharmacodynamics of fish oil: protective effects against prostate cancer in TRAMP mice fed with a high fat western diet. *Asian Pacific J Cancer Prev*. 2011;12:3331-3334.
38. Gunawan S, Aulia A, Soetikno V. Development of rat metabolic syndrome models: a review. *Vet World*. 2021;14(7):1774-1783.
39. Wong SK, Chin KY, Suhaimi FH, Fairus A, Ima-Nirwana S. Animal models of metabolic syndrome: a review. *Nutr Metab*. 2016;13(1):1-12.
40. Weibel E. Principles and methods for the morphometric study of the lung and other organs. *Lab Invest*. 1963;12:131-155.
41. Mateus PAM, Kido LA, Silva RS, Cagnon VHA, Montico F. Association of anti-inflammatory and antiangiogenic therapies negatively influences prostate cancer progression in TRAMP mice. *Prostate*. 2019;79:515-535.
42. Kido LA, Hahm E-R, Kim S-H, et al. Prevention of prostate cancer in transgenic adenocarcinoma of the mouse prostate mice by yellow passion fruit extract and antiproliferative effects of its bioactive compound piceatannol. *J Cancer Prev*. 2020;25:87-99.
43. Lévesque S, Pol JG, Ferrere G, Galluzzi L, Zitvogel L. Trial watch: dietary interventions for cancer therapy. *Oncoimmunology*. 2019;8:1-8.
44. da Silva RF, Nogueira-Pangrazi E, Kido LA, et al. Nintedanib antiangiogenic inhibitor effectiveness in delaying adenocarcinoma progression in transgenic adenocarcinoma of the mouse prostate (TRAMP). *J Biomed Sci*. 2017;24:1-19.
45. Nogueira-Pangrazi E, Silva RF, Kido LA, Montico F, Cagnon HA. Nintedanib antiangiogenic inhibitor effectiveness in delaying adenocarcinoma progression in transgenic adenocarcinoma of the mouse prostate (TRAMP). *Cell Biol Int*. 2018;42:153-168.
46. Zhou Y, Bolton EC, Jones JO. Androgens and androgen receptor signaling in prostate tumorigenesis. *J Mol Endocrinol*. 2015;54:R15-R29.
47. Husain I, Shukla S, Soni P, Husain N. Role of androgen receptor in prostatic neoplasia versus hyperplasia. *J Cancer Res Ther*. 2016;12:112-116.
48. Tamarindo GH, Góes RM. Docosahexaenoic acid differentially modulates the cell cycle and metabolism-related genes in tumor and pre-malignant prostate cells. *Biochim Biophys Acta—Mol Cell Biol Lipids*. 2020;1865(10):158766.
49. Wang S, Wu J, Suburu J, et al. Effect of dietary polyunsaturated fatty acids on castration-resistant Pten-null prostate cancer. *Carcinogenesis*. 2012;33:404-412.
50. Akinsete JA, Ion G, Witte TR, Hardman WE. Consumption of high w-3 fatty acid diet suppressed prostate tumorigenesis in C3(1) Tag mice. *Carcinogenesis*. 2012;33:140-148.
51. Niu Y, Altuwajiri S, Yeh S, et al. Targeting the stromal androgen receptor in primary prostate tumors at earlier stages. *PNAS*. 2008;105:12188-12193.
52. Champeil-Potokar G, Hennebelle M, Latour A, Vancassel S, Denis I. Docosahexaenoic acid (DHA) prevents corticosterone-induced changes in astrocyte morphology and function. *J Neurochem*. 2016;136(6):1155-1167.
53. Simanainen U, Lampinen A, Henneicke H, et al. Long-term corticosterone treatment induced lobe-specific pathology in mouse. *Prostate*. 2011;297(71):289-2977.
54. Zhao B, Choi JP, Jaehne M, et al. Glucocorticoid receptor in prostate epithelia is not required for corticosteroid-induced epithelial hyperproliferation in the mouse. *Prostate*. 2014;1078:1068-1078.
55. Weikum ER, Liu X, Ortlund EA. The nuclear receptor superfamily: a structural perspective. *Protein Sci*. 2018;27:1879-1892.
56. Sideris S, Aoun F, Martinez CN, et al. Role of corticosteroids in prostate cancer progression: implications for treatment strategy in metastatic castration-resistant patients. *J Endocrinol Invest*. 2016;39(7):729-738.

57. Isikbay M, Otto K, Kregel S, Conzen SD, Szmulewitz RZ. Glucocorticoid receptor activity contributes to resistance to androgen-targeted therapy in prostate cancer. *Horm Canc.* 2014;5:72-89.
58. Arora VK, Schenkein E, Murali R, et al. Glucocorticoid receptor confers resistance to antiandrogens by bypassing androgen receptor blockade. *Cell.* 2013;155:1309-1322.
59. Li J, Alyamani M, Zhang A, et al. Aberrant corticosteroid metabolism in tumor cells enables GR takeover in enzalutamide resistant prostate cancer. *eLife.* 2017;6:1-17.
60. Montico F, Kido LA, Martin RS, Rowley DR, Cagnon HA. Reactive stroma in the prostate during late life: the role of microvasculature and antiangiogenic therapy influences. *Prostate.* 2015;1661:1643-1661.
61. Tuxhorn JA, Ayala GE, Rowley DR. Reactive stroma in prostate cancer progression. *J Urol.* 2001;166:2472-2483.
62. Wang C, Luo F, Zhou Y, et al. The therapeutic effects of docosahexaenoic acid on oestrogen/androgen-induced benign prostatic hyperplasia in rats. *Exp Cell Res.* 2016;345:125-133.
63. Yin Y, Sui C, Meng F, Ma P, Jiang Y. The omega-3 polyunsaturated fatty acid docosahexaenoic acid inhibits proliferation and progression of non-small cell lung cancer cells through the reactive oxygen species-mediated inactivation of the PI3K/Akt pathway. *Lipids Health Dis.* 2017;16:1-9.
64. Kajikawa S, Imada K, Takeuchi T. Eicosapentaenoic acid attenuates progression of hepatic fibrosis with inhibition of reactive oxygen species production in rats fed methionine- and choline-deficient diet. *Dig Dis Sci.* 2011;56:1065-1074.
65. Hwang JK, Yu HN, Noh EM, et al. DHA blocks TPA-induced cell invasion by inhibiting MMP-9 expression via suppression of the PPAR- $\gamma$ /NF- $\kappa$ B pathway in MCF-7 cells. *Oncol Lett.* 2017;13:243-249.
66. Silva RS, Kido LA, Montico F, Vendramini-Costa DB, Pilli RA, Cagnon V. Steroidal hormone and morphological responses in the prostate anterior lobe in different cancer grades after celecoxib and goniothalamin treatments in TRAMP mice. *Cell Biol Int.* 2018;42:1006-1020.
67. Fan Y-Y, Ly LH, Barhoumi R, McMurray DN, Chapkin RS. Dietary docosahexaenoic acid suppresses T cell protein kinase C $\theta$  lipid raft recruitment and IL-2 production. *J Immunol.* 2004;173(10):6151-6160.
68. Denys A, Hichami A, Akhtar Khan N. Eicosapentaenoic acid and docosahexaenoic acid modulate MAP kinase enzyme activity in human T-cells. *Mol Cell Biochem.* 2002;232(1-2):143-148.
69. Shinto L, Marracci G, Bumgarner L, Yadav V. The effects of omega-3 fatty acids on matrix metalloproteinase-9 production and cell migration in human immune cells: implications for multiple sclerosis. *Autoimmune Dis.* 2011;1(1):134592.
70. Richardsen E, Uglehus RD, Due J, Busch C, Busund LTR. The prognostic impact of M-CSF, CSF-1 receptor, CD68 and CD3 in prostatic carcinoma. *Histopathology.* 2008;53(1):30-38.
71. Flammiger A, Bayer F, Cirugeda-Kühnert A, et al. Intratumoral T but not B lymphocytes are related to clinical outcome in prostate cancer. *APMIS.* 2012;120:901-908.
72. Adissu HA, McKerlie C, Di Grappa M, et al. Timp3 loss accelerates tumour invasion and increases prostate inflammation in a mouse model of prostate cancer. *Prostate.* 2015;75(16):1831-1843.
73. Kaur HB, Guedes LB, Lu J, et al. Association of tumor-infiltrating T-cell density with molecular subtype, racial ancestry and clinical outcomes in prostate cancer. *Mod Pathol.* 2018;31(10):1539-1552.
74. Xiang P, Jin J. Infiltrating CD4 + T cells attenuate chemotherapy sensitivity in prostate cancer via CCL5 signaling. *Prostate.* 2019;79:1018-1031.
75. Dinicolantonio JJ, Keefe JHO. Effects of dietary fats on blood lipids: a review of direct comparison trials. *Open Hear.* 2018;5:1-5.
76. Innes JK, Calder PC. Marine omega-3 (N-3) fatty acids for cardiovascular health: an update for 2020. *Int J Mol Sci.* 2020;21:1-21.
77. Allott EH, Howard LE, Cooperberg MR, et al. Serum lipid profile and risk of prostate cancer recurrence: results from the SEARCH database. *Am Assoc Cancer Res.* 2014;23:2349-2356.
78. Jamnagerwalla J, Howard LE, Allott EH, et al. Serum cholesterol and risk of high-grade prostate cancer: results from the REDUCE study. *Prostate Cancer Prostatic Dis.* 2018;21:252-259.
79. Arcidiacono B, Iiritano S, Nocera A, et al. Insulin resistance and cancer risk: an overview of the pathogenetic mechanisms. *Exp Diabetes Res.* 2012;2012:2012.
80. Klafke JZ, Porto FG, Batista R, et al. Association between hypertriglyceridemia and protein oxidation and proinflammatory markers in normocholesterolemic and hypercholesterolemic individuals. *Clin Chim Acta.* 2015;448:50-57.
81. Allott EH, Masko EM, Freedland AR, et al. Serum cholesterol levels and tumor growth in a PTEN-null transgenic mouse model of prostate cancer. *Prostate Cancer Prostatic Dis.* 2018;21:196-203.
82. Sun C, Yan ZW. DHA regulates lipogenesis and lipolysis genes in mice adipose and liver. *Mol Biol Rep.* 2011;38:731-737. doi:10.1007/s11033-010-0160-9
83. Jossic-corcous CLE. Hepatic farnesyl diphosphate synthase expression is suppressed by polyunsaturated fatty acids. *Biochem J.* 2005;794:787-794.

**How to cite this article:** Amaro GM, da Silva AD, Tamarindo GH, et al. Differential effects of omega-3 PUFAS on tumor progression at early and advanced stages in TRAMP mice. *The Prostate.* 2022;1-14. doi:10.1002/pros.24421